Chinese Chemical Letters 31 (2020) 984–987

Contents lists available at ScienceDirect

Chinese Chemical Letters

journal homepage: www.elsevier.com/locate/cclet

Communication

Two-dimensional vanadium carbide (V_2CT_x) MXene as supercapacitor electrode in seawater electrolyte

Hongtian He, Qixun Xia*, Bingxin Wang, Libo Wang, Qianku Hu, Aiguo Zhou*

School of Materials Science and Engineering, Henan Polytechnic University, Jiaozuo 454000, China

ARTICLE INFO

Article history:
Received 11 June 2019
Received in revised form 8 August 2019
Accepted 11 August 2019
Available online 16 August 2019

Keywords:
MXene
Two-dimensional carbide
V_2CT_x
Supercapacitor
Seawater

ABSTRACT

In this study, two-dimensional V_2CT_x MXene has been prepared by selectively etching Al layers from V_2AlC MAX phase by NaF+HCl etching at 90 °C for 72 h and its performance as supercapacitor (SC) electrode were tested using simulating seawater as electrolyte. V_2CT_x MXene-based electrodes shows a good capacitance of 181.1 F/g, which is in accordance with the volumetric specific capacitance of 317.8 F/cm^3, and with 89.1% capacitance retention even after 5000 cycle. Compared with other MXenes, V_2CT_x have better electrochemical performance as SC electrode. This work provides an innovative strategy to apply V_2CT_x MXene as SC electrode in safety and effective seawater electrolyte.

Recently, a new family of 2D materials, named MXenes [1], have exhibited various unusual properties compared to previously reported 2D materials like MoS_2 [2–4], graphene [5–8], and phosphorene [9]. These MXenes are synthesized by selective removal of the A layers from a laminar MAX phase material with the structural formula $M_{n+1}AX_n$, where M is an early transition metal, A is mostly IIIA- and IVA-group elements, X is carbon and/or nitrogen, and $n = 1$, 2 or 3 [10,11].

Generally, MXenes were under investigation as electrode materials in lithium-ion batteries (LIB) [12,13] and supercapacitors (SCs) [14–18], because of the unusual properties of MXenes, such as high specific surface area, excellent conductivity and good hydrophilicity [1,19]. Recently, compared with LIBs, SCs have received considerable and growing attention due to their faster charge/discharge rates, high power densities, long cycle lives, and superior reliability [20–26]. Generally, mass capacitance is used to evaluate SC electrode. However, with the increasing requirement for portable energy storage devices, the volumetric capacity is an important parameter for SCs, also [27]. MXenes are being studied as electrode materials in SCs [28,29] with superior volumetric capacitance than carbonaceous electrodes [16,30].

At present, around twenty MXenes, such as $Ti_3C_2T_x$, Ti_2CT_x, and Nb_2CT_x (the T_x represents surface termination groups, such as —OH, —F and —O) were synthesized successfully and widely used as electrode materials for energy storage [31–33]. Recently, Ghidiu *et al.* synthesized a clay-like titanium carbide MXene with high volumetric capacitance of 900 F/cm^3 (245 F/g) at a scan rate of 2 mV/s in 1 mol/L H_2SO_4 electrolyte [30]. Shen *et al.* prepared a $Ti_3C_2T_x$ MXene film electrode by a vacuum-filtrating method exhibited volumetric capacitance of 49.6 F/cm^3 (0.63 A/cm^3) in 1 mol/L H_2SO_4 electrolyte [18]. Lukatskaya *et al.* reported $Ti_3C_2T_x$ MXene electrodes with volumetric capacitance of 340 F/cm^3 (100 F/g) in 1 mol/L KOH electrolyte at a scan rate of 20 mV/s [16]. The previous exploration of MXene mainly focused on $Ti_3C_2T_x$ MXene-based electrode materials. However, there are few reports on V_2CT_x MXene as electrode materials for SC applications. Based on theoretical calculation, V_2CT_x has better electrochemical performance than other MXenes [34], and this theoretical predication was confirmed by experimental results [35,36]. V_2CT_x as one of the promising electrode materials for energy storages due to the unique properties, such as (1) Vanadium is a relatively light atom among all transition metals; (2) Compared with $Ti_3C_2T_x$, V_2CT_x MXene has thinner layer thickness, which leads to a faster ion diffusion rates; (3) V_2CT_x is likely to possess the pseudocapacitive behavior due to the multiple valences of vanadium element.

As LIB anode, V_2CT_x has excellent performance to adsorb and store Li ion [36]. Besides Li ion, it was also reported that V_2CT_x theoretically has excellent performance to adsorb and store K and Na ions [37–39]. Therefore, V_2CT_x should have excellent performance as electrode of SC in an electrolyte solution containing K^+ or Na^+ ions. Shan *et al.* reported a flexible V_2C film in 1 mol/L KOH electrolyte that exhibited a high specific capacitance of 184 F/g [40]. However, most of the electrolyte solutions uses in SCs are consisting of inorganic chemicals like KOH and H_2SO_4 or dangerous toxic organic, thus causing environment problem. Moreover,

* Corresponding authors.
E-mail addresses: xqx@hpu.edu.cn (Q. Xia), zhouag@hpu.edu.cn (A. Zhou).

https://doi.org/10.1016/j.cclet.2019.08.025

organic electrolytes prices in present scenario are comparatively expensive. An aqueous electrolytes based on Na^+, K^+ and Mg^{2+} salts provide low ionic resistivity, fast ion transportation, and hence, can impart safety and economic benefits to SCs [41]. In general, Na^+ ions are abundantly available on earth; therefore, they can be easily obtained from the seawater, which, in fact, contains 0.46 mol/L of NaCl [42]. The SC fabrication process in the simulating seawater solution as the electrolyte solution can be easier and cheaper due to its abundance, electrochemical stability, and environment-friendly character. Herein, we report simulating seawater arbitrated V_2CT_x MXene-based SCs with high volumetric capacitance and good cycling stability. The new member of MXene, V_2CT_x MXene, as promising electrode materials for SC, exhibited wider potential window and higher specific capacitance than other MXenes. However, the V_2CT_x MXene often shows unsatisfactory stability in strong alkaline or acidic electrolytes. Hence, we report simulating seawater arbitrated V_2CT_x MXene-based SCs with high specific capacitance and good cycling stability.

The composition and microstructure of synthesized V_2CT_x MXene are shown in Fig. 1. Fig. 1a is the XRD patterns of V_2AlC before and after NaF+HCl etching. After etching, almost all peaks belong to V_2AlC disappear. The new peak with $2\theta = 8.06^\circ$ is belongs to V_2CT_x MXene. Agree with previous work, the V_2CT_x made by this method is highly pure [43]. In particular, in this study, the traditional HF solution exfoliation was replaced by NaF+HCl etching due to HF has strong causticity and toxicity, and it is easily to damage the structure of MXene. Therefore, NaF+HCl as milder etching solvent was used to etched V_2AlC. In addition, from others research, it was noticed that Ti_3C_2 etched by fluorine salt with HCl has much better electrochemical performance as SC electrodes than that etched by HF solution.

The SEM image of V_2CT_x sample is shown in Fig. 1b. The sample presents a multi-slice layered structure, which is the typical "accordion" structure of MXene. The inset of Fig. 1b is the TEM image of a fully exfoliated V_2CT_x flake, shows a typical 2D structure with a large area and small thickness. The edge of the flake has significant curl, indicating that the V_2CT_x flake is very thin and has a certain toughness. The AFM image of V_2CT_x flakes is shown in Fig. 1c. The thickness of V_2CT_x nanosheets is measured to be 1.7 nm (mono-layer) or 3.4 nm (double layer). The thickness is very close the thickness of Ti_3C_2 mono-layer (1.6 nm) measured by AFM reported by Lipatov *et al.* [44]. Thus the V_2CT_x sheets shown in Fig. 1c are mono-layer or few-layer MXene. Such a layered structure could be advantageous to the electrolyte penetration and electron transfer of V_2CT_x electrode.

The N_2 adsorption-desorption isotherms of this V_2CT_x (not shown for concise) is very similar with that in our previous work [45]. The Brunauer-Emmett-Teller specific surface area (SSA) was estimated to be 19.3 m^2/g. Based on the isothermal and SSA, the V_2CT_x sample had open pore structure and high surface area, which could benefit to its electrochemical performance, as the pore channels facilitate rapid electrolyte diffusion to the surface of the active material. To understand the chemical nature of V_2CT_x MXene, the photoelectron spectroscopy (XPS) spectrum of V_2CT_x MXene were provided in our previous report [36]. From the XPS results, the main ingredients of tested samples can be concluded as V_2CT_x MXene with F/PH/O functional groups. Meanwhile, the XPS results show higher C concentration than the supposed concentration, which leads to better conductivity, further improve the electrochemical performance.

Fig. 2a shows the CV curves of V_2CT_x-based electrode. In Fig. 2a, the shapes of the CV curves are nearly the ideal rectangular shapes, indicative of good cyclic stability. As the scan rate is increased, meanwhile CV profiles still retain a relatively rectangular shape without obvious distortion, exhibiting excellent high rate performance. All CV curves indicate the electrode of V_2CT_x possess the excellent conductivity and have good interfacial contact with the electrolyte, which provide fast ion transport channels for the simulating seawater electrolyte.

Fig. 2b shows the GCD curves of the V_2CT_x electrode in the potential range of −0.8 V to −0.3 V at current density from 0.2 A/g to 3 A/g. In the figure, the nonlinear GCD curves without a plateau show that V_2CT_x stores charge pseudocapacitively. At low current density, the GCD curve of V_2CT_x electrode (Fig. S1 in Supporting information) presents mixed electrical double-layer capacitor (EDLC) and pseudocapacitor behaviors, starting with an EDLC symmetric charge/discharge curve followed by pseudocapacitor discharge status [46]. This is attribute to large surface area of V_2CT_x MXene electrode could produce a significant EDLC capacitance, especially for the highly porous MXene electrode. Thus, the potential rapidly drops by its EDLC capacitive discharge first during the discharge process, followed by the phase transformation plateau with an extended discharge time due to the electrolyte ion diffusion into the inner pores of V_2CT_x MXene for redox reactions. However, with a large current density, the GCDs demonstrated better symmetry mainly due to rapid charge and discharge reduces the redox reactions during the discharge process.

The specific capacitance values calculated from the GCD curves (Fig. 2b) at the current densities of 0.2, 0.5, 1, 2 and 3 A/g were 181.1, 171.4, 91.3, 39.1 and 11.8 F/g, respectively (Fig. 2c). The SC value reached 181.1 F/g at the current density of 0.2 A/g, corresponding to the volumetric specific capacitance of 317.8 F/cm^3, significantly superior than the values of Ti_2CT_x (51 F/g at 1 A/g) electrodes in literature [45]. Even further treatment and complex structure were made to improve the capacitance of Ti_2CT_x or $Ti_3C_2T_x$, as-prepared V_2CT_x still has higher capacitance. Compared with previous theoretical [34] and experimental work [43] on the properties of V_2CT_x as anode of Li-ion batteries, this work shows similar results that V_2CT_x have better electrochemical performance than other MXenes as SC electrode (Table S1 in Supporting information). More research work need be done to understand why V_2CT_x has so better performance. For instance, Shan *et al.* tested the V_2CT_x

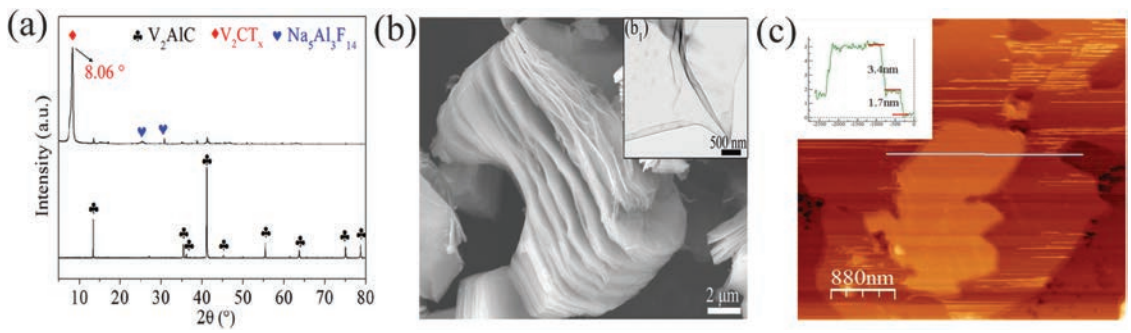

Fig. 1. (a) XRD patterns of V_2AlC and V_2CT_x. (b) SEM and TEM (inset b1) images of V_2CT_x, (c) AFM image of V_2CT_x.

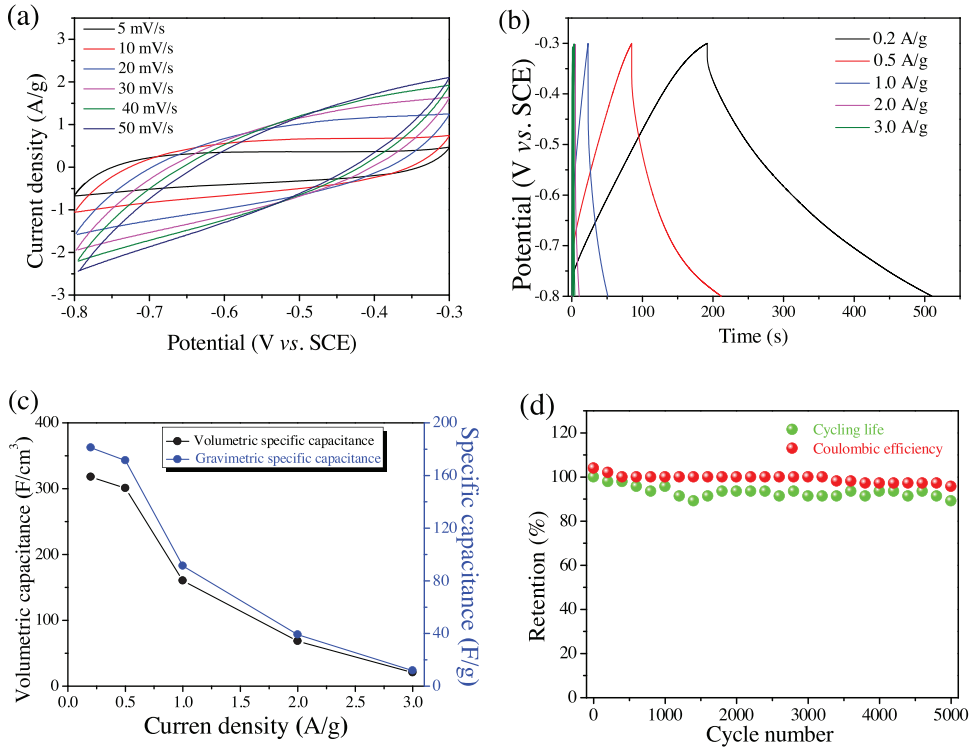

Fig. 2. (a) CV curves and (b) GCD curves of V_2CT_x-based SC. (c) Comparison of the specific gravimetric capacitances and specific volumetric capacitances of the V_2CT_x electrode at different current densities. (d) Cycling performance and Columbic efficiency of the V_2CT_x electrode at current density of 2 A/g.

MXene in 1 mol/L H_2SO_4 electrolyte exhibited very high specific capacitance of 487 F/g at scan rate of 2 mV/s [40]. A possible reason should be because that V_2CT_x's adsorption energy of alkali metal cation is higher than that of other MXenes [47]. In future work, full cells need be fabricated and tested, which will help to show their potential applications in energy storage field.

Electrochemical properties of the V_2CT_x electrode was further characterized by long-term cycling and Columbic efficiency test at a current density of 2 A/g over 5000 cycles (Fig. 2d). The specific capacitance value of the V_2CT_x electrode slowly decreases for the first 1400 cycles and stay stable for the next 3600 cycles with a retention rate 89.1% over the 5000 cycles. This leads to a relatively high Columbic efficiency at current density of 2 A/g after 5000 cycle of ~95.7, which is comparable to those reported $Ti_3C_2T_x$ MXene and $Ti_3C_2T_x$/RGO composite based SCs [48], suggesting a favorable structural soundness, chemical durability and environmental prestige of the V_2CT_x electrode in seawater electrolyte system.

In conclusion, we have successfully produced V_2CT_x MXene with NaF and HCl solution at 90 °C for 72 h. After ultrasonic treatment, The V_2CT_x nanosheets with high SSA (19.3 m^2/g) were made. The V_2CT_x MXene shows a typical "accordion" structure, which is a very favorable microstructure as SC electrodes. The electrochemical measurements show that the V_2CT_x-based SC had the volumetric specific capacitance of 317.8 F/cm^3 at current density of 0.2 A/g, and an excellent cycling stability, *i.e.*, 89.1% capacitance retention after 5000 cycles. From the comparison with other MXenes, it was found that V_2CT_x have better electrochemical performance than other MXenes as SC electrode in seawater electrolyte.

Acknowledgements

This work is supported by the National Natural Science Foundation of China (No. 51772077), Program for Innovative Research Team (in Science and Technology) in the University of Henan Province (No. 19IRTSTHN027), Natural Science Foundation of Henan Province (Nos. 182300410228 and 182300410275), the China Postdoctoral Science Foundation (No. 2019M652537) and Henan Postdoctoral Foundation (No. 19030065).

Appendix A. Supplementary data

Supplementary material related to this article can be found, in the online version, at doi:https://doi.org/10.1016/j.cclet.2019.08.025.

References

[1] M. Naguib, O. Mashtalir, J. Carle, et al., ACS Nano 6 (2012) 1322–1331.
[2] S.P. Zhang, X.Z. Song, S.H. Liu, et al., Electrochim. Acta 312 (2019) 1–10.
[3] M.A. Bissett, I.A. Kinloch, R.A.W. Dryfe, ACS Appl. Mater. Inter. 7 (2015) 17388–17398.
[4] L.J. Cao, S.B. Yang, W. Gao, et al., Small 9 (2013) 2905–2910.
[5] S. Dong, X. He, H. Zhang, et al., J. Mater. Chem. A 6 (2018) 15954–15960.
[6] X. He, N. Zhang, X. Shao, et al., Chem. Eng. J. 297 (2016) 121–127.
[7] X. He, X. Li, H. Ma, et al., J. Power Sources 340 (2017) 183–191.
[8] X. He, H. Zhang, H. Zhang, et al., J. Mater. Chem. A 2 (2014) 19633–19640.
[9] L. Zu, X. Gao, H.Q. Lian, et al., J. Alloys Compd. 770 (2019) 26–34.
[10] M.W. Barsoum, MAX Phases: Properties of Machinable Ternary Carbides and Nitrides, Wiley-VCH, Weinheim, 2013.
[11] M.W. Barsoum, Prog. Solid State Chem. 28 (2000) 201–281.
[12] D. Er, J. Li, M. Naguib, Y. Gogotsi, V.B. Shenoy, ACS Appl. Mater. Interface 6 (2014) 11173–11179.
[13] Q. Tang, Z. Zhou, P. Shen, J. Am. Chem. Soc. 134 (2012) 16909–16916.
[14] X. Wang, T.S. Mathis, K. Li, et al., Nat. Energy 4 (2019) 241.
[15] M.R. Lukatskaya, S. Kota, Z. Lin, et al., Nat. Energy 2 (2017) 17105.
[16] M.R. Lukatskaya, O. Mashtalir, C.E. Ren, et al., Science 341 (2013) 1502–1505.
[17] M.D. Levi, M.R. Lukatskaya, S. Sigalov, et al., Adv. Energy Mater. 5 (2015) 1400815.
[18] B.S. Shen, H. Wang, L.J. Wu, et al., Chin. Chem. Lett. 27 (2016) 1586–1591.
[19] M. Kurtoglu, M. Naguib, Y. Gogotsi, M.W. Barsoum, MRS Commun. 2 (2012) 133–137.
[20] Y. Zhu, S. Murali, M.D. Stoller, et al., Science 332 (2011) 1537–1541.
[21] P. Simon, Y. Gogotsi, Materials for Electrochemical Capacitors, World Scientific, 2010, pp. 320–329.
[22] J. Yan, Q. Wang, T. Wei, Z. Fan, Adv. Energy Mater. 4 (2014) 1300816.

[23] C. Wang, P. Sun, G. Qu, J. Yin, X. Xu, Chin. Chem. Lett. 29 (2018) 1731–1740.
[24] N.M. Shinde, Q.X. Xia, P.V. Shinde, et al., ACS Appl. Mater. Inter. 11 (2019) 4551–4559.
[25] N.M. Shinde, Q.X. Xia, J.M. Yun, et al., Electrochim. Acta 296 (2019) 308–316.
[26] T.F. Zhang, Q.X. Xia, Z. Wan, et al., Chem. Eng. J. 360 (2019) 1310–1319.
[27] M. Ghidiu, M.R. Lukatskaya, M.Q. Zhao, Y. Gogotsi, M.W. Barsoum, Nature 516 (2014) 78–81.
[28] Z. Ling, C.E. Ren, M.Q. Zhao, et al., Proc. Natl. Acad. Sci. U. S. A. 111 (2014) 16676–16681.
[29] R. Rakhi, B. Ahmed, M.N. Hedhili, D.H. Anjum, H.N. Alshareef, Chem. Mater. 27 (2015) 5314–5323.
[30] M. Ghidiu, M.R. Lukatskaya, M.Q. Zhao, Y. Gogotsi, M.W. Barsoum, Nature 516 (2014) 78.
[31] Q.X. Xia, N.M. Shinde, J.M. Yun, et al., Electrochim. Acta 271 (2018) 351–360.
[32] A. Byeon, A.M. Glushenkov, B. Anasori, et al., E. J. Power Sources 326 (2016) 686–694.
[33] Y. Yoon, M. Lee, S.K. Kim, et al., Adv. Energy Mater. 8 (2018) 1703173.
[34] D. Sun, Q. Hu, J. Chen, et al., ACS Appl. Mater. Inter. 8 (2016) 74.
[35] M. Naguib, J. Halim, J. Lu, et al., J. Am. Chem. Soc. 135 (2013) 15966–15969.
[36] F. Liu, J. Zhou, S. Wang, et al., J. Electrochem. Soc. 164 (2017) A709–A713.
[37] C. Eames, M.S. Islam, J. Am. Chem. Soc. 136 (2014) 16270–16276.
[38] Y. Xie, Y. Dall'Agnese, M. Naguib, et al., ACS Nano 8 (2014) 9606–9615.
[39] Y. Dall'Agnese, P.L. Taberna, Y. Gogotsi, P. Simon, J. Phys. Chem. Lett. 6 (2015) 2305–2309.
[40] Q. Shan, X. Mu, M. Alhabeb, et al., Electrochem. Commun. 96 (2018) 103–107.
[41] K. Fic, G. Lota, M. Meller, E. Frackowiak, Energy Environ. Sci. 5 (2012) 5842–5850.
[42] J.K. Kim, E. Lee, H. Kim, et al., ChemElectroChem 2 (2015) 328–332.
[43] Y. Liu, X. Zhang, S. Dong, Z. Ye, Y. Wei, J. Mater. Sci. 52 (2017) 2200–2209.
[44] A. Lipatov, H. Lu, M. Alhabeb, et al., Sci. Adv. 4 (2018) eaat0491.
[45] R.B. Rakhi, B. Ahmed, M.N. Hedhili, D.H. Anjum, H.N. Alshareef, Chem. Mater. 27 (2015) 5314–5323.
[46] J. Xie, P. Yang, Y. Wang, et al., J. Power Sources 401 (2018) 213–223.
[47] Y. Xie, Y. Dall'Agnese, M. Naguib, et al., ACS Nano 8 (2014) 9606–9615.
[48] C.J. Zhao, Q. Wang, H. Zhang, S. Passerini, X.Z. Qian, ACS Appl. Mater. Interface 8 (2016) 15661–15667.